On the sign of the neutrino asymmetry induced by active-sterile neutrino oscillations in the early Universe

P. Di Bari[1] and R. Foot[2]

(1st of December)

[1] *Dipartimento di Fisica, Università di Roma "La Sapienza" and*
I.N.F.N Sezione di Roma 1
P.le Aldo Moro, 2, I00185 Roma, Italy
(dibari@roma1.infn.it)
[2] *School of Physics*
Research Centre for High Energy Physics
The University of Melbourne
Parkville 3052 Australia
(foot@physics.unimelb.edu.au)

Abstract

We deal with the problem of the final sign of the neutrino asymmetry generated by active-sterile neutrino oscillations in the Early Universe solving the full momentum dependent quantum kinetic equations. We study the parameter region $10^{-2} \overset{<}{\sim} |\delta m^2|/eV^2 \leq 10^3$. For a large range of $\sin^2 2\theta_0$ values the sign of the neutrino asymmetry is fixed and does not oscillate. For values of mixing parameters in the region $10^{-6} \overset{<}{\sim} \sin^2 2\theta_0 \overset{<}{\sim} 3 \times 10^{-4} \, (eV^2/|\delta m^2|)$, the neutrino asymmetry appears to undergo rapid oscillations during the period where the exponential growth occurs. Our numerical results indicate that the oscillations are able to change the neutrino asymmetry sign. The sensitivity of the solutions and in particular of the final sign of lepton number to small changes in the initial conditions depends whether the number of oscillations is high enough. It is however not possible to conclude whether this effect is induced by the presence of a numerical error or is an intrinsic feature. As the amplitude of the statistical fluctuations is much lower than the numerical error, our numerical analysis cannot demonstrate the possibility of a chaotical generation of lepton domains. In any case this possibility is confined to a special region in the space of mixing parameters and it cannot spoil the compatibility of the $\nu_\mu \leftrightarrow \nu_s$ solution to the neutrino atmospheric data obtained assuming a small mixing of the ν_s with an $eV - \tau$ neutrino.

I. INTRODUCTION

If light sterile neutrinos exist, then this will lead to important implications for early Universe cosmology. This is because ordinary-sterile neutrino oscillations generate large neutrino asymmetries for the large range of parameters, $\delta m^2 \gtrsim 10^{-5} \ eV^2$, $\sin^2 2\theta_0 \gtrsim 10^{-10}$ [1–7]. This is a generic feature of ordinary-sterile neutrino oscillations for this parameter range. For $\delta m^2 \lesssim 10^{-5} \ eV^2$, the evolution of neutrino asymmetry is qualitatively quite different as collisions are so infrequent and a large neutrino asymmetry cannot be generated [8,9]. Interestingly, some people do not currently accept that large neutrino asymmetry is generated in the early Universe [10]. We will comment briefly on this later in the paper.

An important issue which has yet to be fully addressed is the sign of this asymmetry. Is it always fixed or can it be random? This is an important issue because a random asymmetry may lead to domains with lepton number of different signs [1]. If such domains exist then this may lead to observable consequences. For example, active neutrinos crossing the boundaries of these lepton domains could undergo a MSW resonance which would lead to a new avenue of sterile neutrino production [11]. In Refs. [12–14] the issue of sign of the asymmetry was discussed in the approximation that all of the neutrinos have the same momentum (i.e. $p = 3.15T$ instead of the Fermi-Dirac distribution). This approximation is not suitable for discussing the temperature region where the exponential growth in neutrino asymmetry occurs. The reason is that in the average momentum toy-model, all of the neutrinos enter the MSW resonance at the same time which significantly enhances the rate at which neutrino asymmetry is created at $T = T_c$. The rapid creation of neutrino asymmetry significantly reduces the region where the oscillations are adiabatic [2].

Thus it is clear that the neutrino momentum dependence must be properly taken into account. This was done in Ref. [2] where an approximate solution to the quantum kinetic equations was derived. This approximate solution was called the 'static approximation' and was re-derived in a different way in Ref. [5] where it was shown that this approximation was just the adiabatic limit of the quantum kinetic equations (QKE's) in the region where lepton number generation is dominated by collisions. Anyway, in the limit where this approximation is valid, it was shown in Ref. [2] that the sign is completely fixed. The static approximation is valid for a large range of parameters but is not valid for large $\sin^2 2\theta_0 \gtrsim 10^{-6}$, $\delta m^2 \sim -10 \ eV^2$. It breaks down in this region because the neutrino asymmetry is generated so rapidly during the exponential growth phase that the quantum kinetic equations are no longer adiabatic. Thus, while Ref. [2] partially answers the question of sign, it does not give the complete answer. The purpose of this paper is to examine the issue of the sign of the asymmetry by numerically solving the quantum kinetic equations.

The outline of this paper is as follows: In section 2 we present some necessary preliminary discussion on active-sterile neutrino oscillations in the early Universe. In section 3 we examine the likely size of the statistical fluctuations in the early Universe. In section 4 we describe the numerical results of our study of the region of parameter space where the sign of the neutrino asymmetry is fixed. Using the results of section 3, we are able to conclude that in this region the statistical fluctuations cannot have any effect and the generated lepton number would have the same sign in all the points of space. In section 5 we describe the features of the transition from the region with no oscillations to one where the

neutrino asymmetry oscillates for a short period during the exponential growth. In section 6 we conclude. Also included is an appendix giving some numerical details, which we hope will be useful to other workers in the field such as the authors of Ref. [10].

II. PRELIMINARY DISCUSSION

Our notation/convention for ordinary-sterile neutrino two state mixing is as follows. The weak eigenstates ν_α ($\alpha = e, \mu$ or τ) and ν_s are linear combinations of two mass eigenstates ν_a and ν_b,

$$\nu_\alpha = \cos\theta_0 \nu_a + \sin\theta_0 \nu_b, \ \ \nu_s = -\sin\theta_0 \nu_a + \cos\theta_0 \nu_b, \tag{1}$$

where θ_0 is the vacuum mixing angle. We define θ_0 so that $\cos 2\theta_0 > 0$ and we adopt the convention that $\delta m^2_{\alpha\beta'} \equiv m_b^2 - m_a^2$. Recall that the α-type neutrino asymmetry is defined by

$$L_{\nu_\alpha} \equiv \frac{n_{\nu_\alpha} - n_{\overline{\nu}_\alpha}}{n_\gamma}. \tag{2}$$

In the above equation, n_γ is the number density of photons. Note that when we refer to "neutrinos", sometimes we will mean neutrinos and/or antineutrinos. We hope the correct meaning will be clear from context. Also, if neutrinos are Majorana particles, then technically they are their own antiparticle. Thus, when we refer to "antineutrinos" we obviously mean the right-handed helicity state in this case.

The density matrix [15,16] for an ordinary neutrino, ν_α ($\alpha = e, \mu, \tau$), of momentum p oscillating with a sterile neutrino in the early Universe can be parameterized as follows:

$$\rho_{\alpha\beta'}(p) = \frac{1}{2}[P_0(p)I + \mathbf{P}(p) \cdot \sigma], \quad \overline{\rho}_{\alpha\beta'}(p) = \frac{1}{2}[\overline{P}_0(p)I + \overline{\mathbf{P}}(p) \cdot \sigma], \tag{3}$$

where I is the 2×2 identity matrix, the "polarisation vector" $\mathbf{P}(p) = P_x(p)\hat{\mathbf{x}} + P_y(p)\hat{\mathbf{y}} + P_z(p)\hat{\mathbf{z}}$ and $\sigma = \sigma_x\hat{\mathbf{x}} + \sigma_y\hat{\mathbf{y}} + \sigma_z\hat{\mathbf{z}}$, with σ_i being the Pauli matrices. It will be understood that the density matrices and the quantities $P_i(p)$ also depend on time t or, equivalently, temperature T. The time-temperature relation for $m_e \stackrel{<}{\sim} T \stackrel{<}{\sim} m_\mu$ is $dt/dT \simeq -M_P/5.44T^3$, where $M_P \simeq 1.22 \times 10^{22}$ MeV is the Planck mass.

We will normalise the density matrices so that the momentum distributions of $\nu_\alpha(p)$ and $\nu_s(p)$ are given by

$$f_{\nu_\alpha}(p) = \frac{1}{2}[P_0(p) + P_z(p)]f_0(p), \quad f_{\nu_s}(p) = \frac{1}{2}[P_0(p) - P_z(p)]f_0(p), \tag{4}$$

where

$$f_0(p) \equiv \frac{1}{1 + \exp\left(\frac{p}{T}\right)}, \tag{5}$$

is the Fermi-Dirac distribution (with zero chemical potential). Similar expressions pertain to antineutrinos (with $\mathbf{P}(p) \rightarrow \overline{\mathbf{P}}(p)$ and $P_0 \rightarrow \overline{P}_0$). The evolution of $\mathbf{P}(p), P_0(p)$ (or $\overline{\mathbf{P}}(p), \overline{P}_0(p)$) are governed by the equations [15–17,5]

3

$$\frac{d\mathbf{P}}{dt} = \mathbf{V}(x) \times \mathbf{P}(x) - D(x)[P_x(x)\hat{\mathbf{x}} + P_y(x)\hat{\mathbf{y}}] + \frac{dP_0}{dt}\hat{\mathbf{z}},$$

$$\frac{dP_0}{dt} \simeq \Gamma(x)\left[\frac{f^{eq}(x)}{f_0(x)} - \frac{1}{2}(P_0(x) + P_z(x))\right], \tag{6}$$

where $D(x) = \Gamma(x)/2$ and $\Gamma(x)$ is the total collision rate of the weak eigenstate neutrino of adimensional momentum $x \equiv p/T$ with the background plasma[1] and $f_{eq}(x)$ is the Fermi-Dirac distribution:

$$f_{eq}(x) \equiv \frac{1}{1 + \exp(x - \tilde{\mu}_\alpha)}. \tag{7}$$

where $\tilde{\mu}_\alpha \equiv \mu_{\nu_\alpha}/T$. For anti-neutrinos, $\tilde{\mu}_\alpha \to \tilde{\mu}_{\bar{\alpha}} \equiv \mu_{\bar{\nu}_\alpha}/T$. The chemical potentials μ_{ν_α}, $\mu_{\bar{\nu}_\alpha}$, depend on the neutrino asymmetry. In general, for a distribution in thermal equilibrium

$$L_{\nu_\alpha} = \frac{1}{4\zeta(3)}\int_0^\infty \frac{x^2 dx}{1 + e^{x - \tilde{\mu}_\alpha}} - \frac{1}{4\zeta(3)}\int_0^\infty \frac{x^2 dx}{1 + e^{x - \tilde{\mu}_{\bar{\alpha}}}}, \tag{8}$$

where $\zeta(3) \simeq 1.202$ is the Riemann zeta function of 3. Expanding out the above equation,

$$L_{\nu_\alpha} \simeq \frac{1}{24\zeta(3)}\left[\pi^2(\tilde{\mu}_\alpha - \tilde{\mu}_{\bar{\alpha}}) + 6(\tilde{\mu}_\alpha^2 - \tilde{\mu}_{\bar{\alpha}}^2)\ln 2 + (\tilde{\mu}_\alpha^3 - \tilde{\mu}_{\bar{\alpha}}^3)\right], \tag{9}$$

which is an exact equation for $\tilde{\mu}_\alpha = -\tilde{\mu}_{\bar{\alpha}}$, otherwise it holds to a good approximation provided that $\tilde{\mu}_{\alpha,\bar{\alpha}} \lesssim 1$. For $T \gtrsim T_{dec}^\alpha$ (where $T_{dec}^e \approx 2.5$ MeV and $T_{dec}^{\mu,\tau} \approx 3.5$ MeV are the chemical decoupling temperatures), $\mu_{\nu_\alpha} \simeq -\mu_{\bar{\nu}_\alpha}$ because processes such as $\nu_\alpha + \bar{\nu}_\alpha \leftrightarrow e^+ + e^-$ are rapid enough to make $\tilde{\mu}_\alpha + \tilde{\mu}_{\bar{\alpha}} \simeq \tilde{\mu}_{e^+} + \tilde{\mu}_{e^-} \simeq 0$. However, for $1 MeV \lesssim T \lesssim T_{dec}^\alpha$, weak interactions are rapid enough to approximately thermalise the neutrino momentum distributions, but not rapid enough to keep the neutrinos in chemical equilibrium [2]. In this case, the value of $\tilde{\mu}_\alpha$ is approximately frozen at $T \simeq T_{dec}^\alpha$ (taking for definiteness $L_{\nu_\alpha} > 0$), while the (negative) anti-neutrino chemical potential $\tilde{\mu}_{\bar{\alpha}}$ continues decreasing until $T \simeq 1$ MeV.

The quantity $\mathbf{V}(x)$ is given by [16,17]

$$\mathbf{V}(x) = \beta(x)\hat{\mathbf{x}} + \lambda(x)\hat{\mathbf{z}}, \tag{10}$$

where $\beta(x)$ and $\lambda(x)$ are

$$\beta(x) = \frac{\delta m^2}{2xT}\sin 2\theta_0, \ \ \lambda(x) = -\frac{\delta m^2}{2xT}[\cos 2\theta_0 - b(x) \pm a(x)], \tag{11}$$

---

[1] From Ref. [18,5] it is given by $\Gamma(x) = yG_F^2 T^5 x$ where $y \simeq 1.27$ for $\nu = \nu_e$ and $y \simeq 0.92$ for $\nu = \nu_\mu, \nu_\tau$ (for $m_e \lesssim T \lesssim m_\mu$).

[2]The chemical and thermal decoupling temperatures are so different because the inelastic collision rates are much less than the elastic collision rates. See e.g. Ref. [18] for a list of the collision rates.

in which the $+(-)$ sign corresponds to neutrino (anti-neutrino) oscillations. The dimensionless variables $a(x)$ and $b(x)$ contain the matter effects [19] (more precisely they are the matter potential divided by $\delta m^2/2xT$). For $\nu_\alpha \to \nu_s$ oscillations $a(x), b(x)$ are given by [20,21]

$$a(x) \equiv \frac{-4\zeta(3)\sqrt{2}G_F T^4 L^{(\alpha)} x}{\pi^2 \delta m^2}, \; b(x) \equiv \frac{-4\zeta(3)\sqrt{2}G_F T^6 A_\alpha x^2}{\pi^2 \delta m^2 M_W^2}, \tag{12}$$

where G_F is the Fermi constant, M_W is the $W-$boson mass, $A_e \simeq 17$ and $A_{\mu,\tau} \simeq 4.9$ (for $m_e \lesssim T \lesssim m_\mu$). The important quantity $L^{(\alpha)}$ is given by the following expression:

$$L^{(\alpha)} \equiv L_{\nu_\alpha} + L_{\nu_e} + L_{\nu_\mu} + L_{\nu_\tau} + \eta \equiv 2L_{\nu_\alpha} + \tilde{L}, \tag{13}$$

where η is a small term due to the asymmetry of the electrons and nucleons and is expected to be very small, $|\eta| \sim 5 \times 10^{-10}$. We will refer to $L^{(\alpha)}$ as the *effective total lepton number* (for the α-neutrino species) since it really needs a name. Note that the quantity $\tilde{L}$ is independent of L_{ν_α} and its value is currently unknown, but could presumably be calculated within a model of baryo-leptogenesis[3]. For our numerical work we took two different values $\tilde{L} = 5 \times 10^{-10}$ and $\tilde{L} = 5 \times 10^{-11}$; in this way we could verify that the final value of the total lepton number does not depend on this particular choice. The neutrino asymmetry L_{ν_α}, on the other hand, evolves dynamically and is a function of $\mathbf{P}, P_0$ and $\bar{\mathbf{P}}, \bar{P}_0$. The equations Eq.(6) constitute a closed set of differential equations for the 8 distributions $\mathbf{P}, P_0, \bar{\mathbf{P}}, \bar{P}_0$. The 'initial' conditions (for $T \to \infty$) are simply $P_x = P_y = 0$, $P_0 = P_z = 1$, assuming here for simplicity that initially $L_{\nu_\alpha} = 0$ (and similarly for antiparticles). Note that the vanishing of $P_{x,y}$ is just an example of the quantum Zeno effect.

From a computational point of view it is useful to write down an explicit differential equation for the neutrino asymmetry to be solved together (see also [4]). This can be done considering that $dL_{\nu_\alpha}/dt = -dL_{\nu_s}/dt$ and, using the Eq.(4), one easily gets:

$$\frac{dL_{\nu_\alpha}}{dt} = \frac{1}{8\zeta(3)} \int \beta(x)[P_y(x) - \bar{P}_y(x)] f_0(x)\, x^2 dx. \tag{14}$$

We mainly employ the useful time saving approximation of integrating the oscillation equations, Eq.(6) [and obviously also Eq.(14)] in the region around the MSW resonances. A detailed description of the numerical procedures is given in the Appendix. Actually away from the resonance the oscillations are typically suppressed by the matter effects or by $\sin^2 2\theta_0$ (or both). Thus, this should be a good approximation, which we carefully checked by taking larger slices of momentum space around the resonance (an example of this check is given in the Appendix).

Before we finish this section we would like to briefly comment on the static approximation [2,5]. The static approximation can be derived by solving the Quantum kinetic equations in the adiabatic limit and assuming that the evolution is dominated by collisions. The resulting

---

[3]Alternatively, it maybe set by divine intervention.

equations are equivalent to keeping the differential equations for $P_0, P_z, \bar{P}_0, \bar{P}_z$ [contained in Eq.(6)] which are functions of $P_y, \bar{P}_y$ which are given by

$$P_y = \frac{-P_z \beta D}{D^2 + \beta^2 + \lambda^2},\tag{15}$$

and $\bar{P}_y$ is similar to the above equation except for the obvious replacement of $P_z \to \bar{P}_z$ and $a \to -a$ in the definition of λ. The evolution of L_{ν_α} is obtained from Eq.(14) above. Numerically, the static approximation is much easier to solve, but it is not always a valid approximation. It is not valid at low temperatures where coherent MSW transitions are important. Also, if the neutrino asymmetry is created fast enough during the exponential growth phase then it may not always be valid (which is the case for $\delta m^2 \sim -10 \ eV^2$ and $\sin^2 2\theta_0 \gtrsim 10^{-6}$, for example). In **figures 1-3**, we give some numerical examples. For **fig. 1a** we take $\nu_\tau \leftrightarrow \nu_s$ oscillations for the parameter choices $\delta m^2 = -10 \ eV^2$, $\sin^2 2\theta_0 = 10^{-7}$. Shown is the evolution of the effective total lepton number, $L^{(\tau)}$, with the solid line representing the numerical solution of the quantum kinetic equations integrating around the resonances [4]. The dashed line is the static approximation discussed above integrating also around the resonances. Observe that there is exact agreement between the QKEs and the static approximation when both are integrated around the resonances, except at low temperatures where the static approximation is not valid, as the evolution there is dominated by coherent oscillations (MSW effect) as discussed in detail in Ref. [3]. In **fig.1b** we compare the static approximation integrating around the resonance with the static approximation integrating over the entire momentum range (which we approximate to $0.01 < p/T < 20$). There is some differences between the static approximation integrated over the entire momentum range with the static approximation (or QKE's) integrated around the resonances. The difference at high temperature can be qualitatively understood because the resonances at high temperature occur at very low momentum, $p_{res}/T \lesssim 1$ where there are very few neutrinos. Thus, the region around $p_{res}/T \sim 2$ can be somewhat important despite being away from the resonance because of the larger number of neutrinos. Also note that the point where the exponential growth occurs is modified slightly, but the rate of growth (the slope) is approximately unmodified. Whether or not there are oscillations of sign depends on the rate at which lepton number is being created during the exponential growth (small changes in the value of T_c would not matter). For this reason, the approximation of integrating around the resonance should be an acceptable approximation.

Figures 2a,b are the same as figure 1a,b except for the different choice of parameters, $\delta m^2 = -100 \ eV^2$, $\sin^2 2\theta_0 = 10^{-8}$.

As a final check of that static approximation we numerically solve the QKEs for the entire momentum range $(0.1 < p/T < 12.0)$ for one example. This is quite CPU time consuming and it is most economically done for small δm^2. We take $\delta m^2 = -0.01 \ eV^2$ and $\sin^2 2\theta_0 = 10^{-7}$. For these parameters, **figure 3** compares the numerical solution of the QKE with the static approximation, both integrated over the entire momentum range. Note

---

[4]Note that at low temperatures $T \lesssim 5 \ MeV$ the repopulation must be taken into account over the entire momentum range, $0.01 < p/T < 20$.

that only the high temperature evolution is shown. As the figure shows we obtain excellent agreement as we expect [5].

Interestingly, Ref. [10] appears to have (almost) rederived the static approximation (they neglect the chemical potentials in the repopulation, which is important for the issue of sign). They seem to get a quite different numerical solution when they numerically solve the static approximation, and are not able to obtain any solution at all when they numerically solve the QKE's. In our opinion, the remarkable agreement between our solution of the static approximation and the QKE's (as figures 1-3 illustrate) is a convincing check that we have done the numerical work competently. Of course this check has been done previously, and there are examples already given in the literature [3], but since this work was ignored in Ref. [10], we have taken the trouble to emphasise it again here.

III. STATISTICAL FLUCTUATIONS

In this section we want to provide a simple estimation of the statistical fluctuations in the effective total lepton number. These arise simply because of the fluctuations in the number of particles within the region, around each oscillating neutrino wavepacket, that determines the properties of the medium through the effective potential.

Let us first proceed without specifying the size of this region but we write it in units of the interaction length $\ell_{int} \equiv \Gamma^{-1}$ of the oscillating neutrino with $x \simeq 2.2$ (the peak of the distribution). The number of photons within a region of size ℓ at the temperature T is given by:

$$N_\gamma \sim n_\gamma \ell^3 \sim 10^{65} \left(\frac{\text{MeV}}{T}\right)^{12} \left(\frac{\ell}{\ell_{int}}\right)^3. \tag{16}$$

Since the number of neutrinos is of the same order as the number of photons, it follows that the statistical fluctuation of lepton number is of order:

$$\Delta L = \frac{\sqrt{N_\nu}}{N_\nu} \sim 10^{-32} \left(\frac{T}{\text{MeV}}\right)^6 \left(\frac{\ell}{\ell_{int}}\right)^{-\frac{3}{2}}. \tag{17}$$

Note that since $n_B \sim 10^{-10} n_\gamma$, it follows that $\Delta\eta = \sqrt{n_B}/n_\gamma \sim 10^{-5}\Delta L$ and thus $\Delta L^{(\alpha)} \sim \Delta L$.

We are interested to evaluate this fluctuation at the critical temperature T_c, when the lepton number starts to be generated. The critical temperature can be put in the following approximated form [2,6]

$$T_c \approx \left(\frac{|\delta m^2|}{\text{eV}^2}\right)^{\frac{1}{6}} 18 \text{ MeV}. \tag{18}$$

---

[5]In the appendix we give further details about the approximation of integrating around the resonance. We also compare the two different numerical procedures employed.

We can thus more usefully express the temperature in units of T_c in Eq. (17), obtaining:

$$\Delta L^{(\alpha)} \simeq 10^{-24} \left(\frac{T}{T_c}\right)^6 \frac{|\delta m^2|}{\text{eV}^2} \left(\frac{\ell}{\ell_{int}}\right)^{-\frac{3}{2}}. \qquad (19)$$

Now what should we take for the size ℓ? We will present a heuristic argument that $\ell \gtrsim 10^{-2}\ell_{int}$. First of all, we find numerically that neutrino asymmetries are typically not significantly created on time scales less than of order $10^{-2}\ell_{int}$ i.e. $\ell_{int}\frac{dL}{dt} \lesssim \mathcal{O}(10^2 L)$ for the parameter space of interest (this is true even in the exponential growth phase). This means that we only need to consider *time* scales greater than $10^{-2}\ell_{int}$. Furthermore since neutrinos are free streaming on such small time scales it follows that the *distance* scale for the creation of L is greater than $10^{-2}\ell_{int}$. Thus the characteristic volume relevant for statistical fluctuations is larger than or of order $(10^{-2}\ell_{int})^3$. Hence, for $|\delta m^2| \leq 1000$ eV^2 we conclude that:

$$\Delta L^{(\alpha)} \lesssim \mathcal{O}\left(10^{-18}\right). \qquad (20)$$

In the next sections we will have to find out whether such fluctuations are able to induce a random sign of the final lepton number. Note that in addition to statistical fluctuations, it is also possible to envisage inhomogeneities which may arise from a model of lepto-baryogenesis for example. Such inhomogeneities may potentially be much larger than the statistical fluctuations but are of course model dependent. Note that the possibility of such inhomogeneities has recently been considered in Ref. [22] where it is shown how the diffusion process must be taken into account to properly describe the dynamical evolution of the neutrino asymmetry.

IV. REGION WITH NO OSCILLATIONS

In Ref. [2] it was shown that in the framework of the static approximation the sign of the final value of total lepton number is the same as the sign of baryon asymmetry term, $\tilde{L}$, and this is due to the presence of a correcting term into the equation (see also Ref. [22] for a detailed discussion). Furthermore, if the initial value of the effective total lepton number is the same as that of $\tilde{L}$, then the effective total lepton number never changes sign during its evolution [otherwise it changes sign only once]. We will simply refer to this situation as *no oscillations*.

In Ref. [2,5] it was also shown that for small mixing angles and $|\delta m^2| \gtrsim 10^{-5}$eV^2, one expects the static approximation to be valid. In this section we present the results of a systematic research in the space of mixing parameters that confirm this expectation. This research has been done solving numerically the QKE. The repopulation term has been taken into account in two different ways.

In the first one we simply describe the active neutrino distribution assuming a thermal distribution ($f_{\nu_\alpha} = f_{eq}$). This assumption is equivalent to saying that the collisions are able to instantaneously refill the states depleted by the oscillations. Such an assumption is justified considering that for temperatures $T \gg 1$MeV (which is typically the case since the region where the sign is determined is during the period of exponential growth which occurs for $T_c \gtrsim 3\ MeV$ for $\delta m^2 \gtrsim 10^{-5}\ eV^2$) and values of $s^2 \ll 10^{-4}$, one has respectively $\Gamma \gg H$

and $\Gamma \gg \Gamma_{\nu_\alpha \to \nu_s}$. In this case in the equations (6) it is approximately valid to replace P_0 and P_z with the neutrino distributions $z_\alpha \equiv f_{eq}/f_0$ and $z_s \equiv f_{\nu_s}/f_0$, via:

$$P_0 = z_\alpha + z_s, \ \ P_z = z_\alpha - z_s. \tag{21}$$

The differential equation for P_z gives a differential equation for z_s

$$\frac{dz_s(x)}{dt} = -\frac{1}{2}\beta(x)\,P_y(x). \tag{22}$$

The differential equation for P_0 becomes redundant because simply:

$$\frac{dP_0}{dt} = \frac{dz_s}{dt} + \frac{dz_\alpha}{dt}, \tag{23}$$

with $z_\alpha \equiv f_{eq}/f_0$, fully determined by the thermal equilibrium assumption [6].

In the second way we calculated the repopulation term using the repopulation equation in Eq.(6). The comparison shows nice agreement, as illustrated in **fig. 4a,b**. Figure 4a is for the parameter choice $\delta m^2 = -1\ eV^2$, $\sin^2 2\theta_0 = 10^{-7}$, while figure 4b is for $\delta m^2 = -10\ eV^2$, $\sin^2 2\theta_0 = 10^{-7}$. The solid line is the numerical integration of the QKEs, Eq.(6) while the dashed line assumes the thermal active neutrino distribution (discussed above). Note that the two computations were done quite independently using different codes. Also, two different initial values of $L^{(\tau)}$ were chosen along with a slightly different initial temperature. We have also done many other examples which we do not show for environmental reasons (i.e. to save trees). This confirms the expectations about the validity of a thermal equilibrium assumption. Note that we only show the *high* temperature evolution since this is the region where the sign is determined. (Recall that the final magnitude of the neutrino asymmetry is in the range $0.23 \stackrel{<}{\sim} L_{\nu_\alpha} \simeq L^{(\alpha)}/2 \stackrel{<}{\sim} 0.37$ as illustrated in figures 1a,2a and is discussed in detail in Ref. [3]).

For fixed values of $|\delta m^2|$, we studied the evolution of lepton number for increasing values of the mixing angle. In the **figure 5** we show an example $\delta m^2 = -10\,\mathrm{eV}^2$. It appears evident that for the shown values of mixing angles, the sign of lepton number does not oscillate. As we will discuss later on, for small mixing angles this result is expected. Of course changing the initial conditions does not change this result as we illustrate in **figure 6** [7]. This figure

---

[6] A naive interpretation of the equation (6) for P_0, would suggest that in the limit of thermal equilibrium $dP_0/dt = 0$. This result is clearly incorrect because on the contrary it corresponds to the case that interactions are off and repopulation is not active at all. The assumption of thermal equilibrium physically corresponds to the case that the rate $\Gamma(x)$ of the collisions, that are refilling the states of momentum x, is so strong that the difference $f_{\nu_\alpha} - f_{\nu_{eq}}$ is very small. Thus it corresponds to the limit $\Gamma \to \infty$ with dP_0/dt finite given by the Eq. (23), from which it follows that $f_{\nu_\alpha} \to f_{\nu_{eq}}$.

[7] Of course qualitatively different behaviour does occur if the initial value of L_{ν_τ} is large enough, roughly, $L_{\nu_\tau}^{initial} \stackrel{>}{\sim} 10^{-5}$ [21,23]. For such a large initial value, the oscillations cannot effectively destroy $L^{(\tau)}$ and $L^{(\tau)}$ remains of order $L_{\nu_\tau}^{initial}$ until lower temperatures where it eventually further increases.

considers $\nu_\tau \leftrightarrow \nu_s$ oscillations with $\delta m^2 = -10\ eV^2$ and $\sin^2 2\theta_0 = 10^{-7}$ with four different initial values of L_{ν_τ} employed.

The result of our careful study of the sign of the neutrino asymmetry is given in **fig. 7**. As the figure shows, the parameter space breaks up into two regions, a no oscillation region and an oscillation region. Looking at the no oscillation region, one can easily identify two different parts, one part at low $\sin^2 2\theta_0$:

$$\sin^2 \stackrel{<}{\sim} 10^{-6}, \tag{24}$$

and one part at large $\sin^2 2\theta_0$,

$$\sin^2 2\theta_0\, \delta m^2 \stackrel{>}{\sim} 3 \times 10^{-4}\, eV^2. \tag{25}$$

The existence of the no oscillation region at low $\sin^2 2\theta_0$ is consistent with the physical insight provided by the static approximation approach. Recall that in this approximation, oscillations of sign do not occur [2,6]. Furthermore this approximation is valid for $\sin^2 2\theta_0$ sufficiently small. This is because the rate of change of lepton number during the exponential growth epoch increases proportionally with the value of $\sin^2 2\theta_0$.

In the region of large $3 \times 10^{-4} eV^2/\delta m^2 \stackrel{>}{\sim} \sin^2 2\theta_0 \stackrel{>}{\sim} 10^{-6}$ oscillations evidently arise at the critical temperature. This is not inconsistent with the static approximation, since it is not valid in this region. At the moment we do not have a clear analytic description of the onset of rapid oscillations, since the QKE's themselves do not provide much physical insight. We can give however a qualitative partial explanation noticing that for $a \ll b$ [recall that a, b are defined in Eq.(12)],

$$\beta/D\big|_{res} \simeq 50 \sin 2\theta_0. \tag{26}$$

Thus, the line $\sin^2 2\theta_0 \approx$ constant (10^{-6}) also corresponds to $\beta/D \approx$ constant (10^{-1}) at the resonance. At the resonance the quantity β/D gives approximately the value of the ratio between the mean interaction length and the matter oscillation length. Until this quantity is much less than unity the coherent behaviour of neutrino oscillations at the resonance is averaged out by the effect of collisions and the static approximation provides a good description for the evolution of the neutrino asymmetry. When this quantity starts to approach unity this starts to be not true any more. Thus, during the initial exponential growth, it is possible that some small effect due to the oscillations between collisions, which is an effect not included in the static approximation, may be responsible for the rapid oscillations of the neutrino asymmetry.

Of course one may wonder why the oscillation region stops when the mixing angle becomes large enough, Eq.(25). Actually there is quite a simple explanation for this result. For large mixing angles such as these, it is known that the exponential generation of lepton number is delayed because of the sterile neutrino production [2,6]. At the same time, the initial exponential growth is considerably weaker. A consequence of the initial slow exponential growth of lepton number the static approximation is valid and oscillations in the sign of lepton number cannot occur while the neutrino asymmetry is growing relatively slowly. Thus this seems to explain why the no oscillation region can extend also to large mixing angles. Infact, in **fig. 8** we show how for $|\delta m^2| = 10^{2.7}\, eV^2$ the critical temperature is delayed

and the rate of growth decreased just when the oscillations would be expected to appear at $s^2 \simeq 10^{-6}$. This is surely the reason why for $|\delta m^2| \gtrsim 10^{2.7}\,\text{eV}^2$, the oscillations do not occur for any value of mixing angle. On the other hand for a fixed value of $|\delta m^2| \lesssim 10^{2.7}\,\text{eV}^2$ the oscillations can occur between $s^2 \simeq 10^{-6}$ and $s^2 \simeq 3 \times 10^{-4}\,(\text{eV}^2/|\delta m^2|)$.

We have now to discuss whether the presence of statistical fluctuations with the amplitude estimated in section III, can give any effect in the "no oscillations" region.

In the static approximation framework, one can show the existence of an approximate fixed point, that for $T > T_c$ is stable and drives the effective total lepton number - $L^{(\alpha)}$ to values of order $10^{-15} - 10^{-16}$ prior to the onset of the instability (see [22]). This is clearly confirmed looking at the solutions in **figures 1-6** and **8**, obtained solving directly the QKEs.

Therefore, from our estimation of the maximum amplitude of the statistical fluctuations, Eq.(20), we can safely exclude any influence of them in determining the final sign of lepton number. We can thus conclude that *for values of mixing parameters in the region where the lepton number does not oscillate, given a certain fixed value of $\tilde{L}$, the final sign of lepton number is the same as that of $\tilde{L}$ and cannot randomly change in different spatial points of the early universe.*

In **fig. 7** we have also showed the contour (dot-dashed line plus the dotted line) of the allowed region for the solution $\nu_\mu - \nu_s$ to the atmospheric neutrino anomaly, in the 3 neutrino mixing mechanism proposed in [2] and reanalyzed in [4,6]. Even assuming that an overproduction of sterile neutrinos would occur in the parameter region of rapid oscillations, as claimed in [11], it appears evident that *the mechanism can still allow acceptable values of the tau neutrino mass and is not inconsistent with standard BBN.*

We want now to investigate more in detail the nature of the rapid oscillations.

V. REGION OF RAPID OSCILLATIONS

The study of the rapid oscillation region is much harder from a numerical point of view. It means that to describe it properly the numerical account of momentum dependence must be much more accurate (on this point more details are given in the numerical Appendix). In particular a much higher resolution in momentum space is necessary to describe the distributions. This makes difficult a systematic exploration of this region for different values of mixing parameters.

We mainly performed the runs for $\delta m^2 = -10\,\text{eV}^2$, a particularly interesting value for the three neutrino mixing mechanism mentioned at the end of previous section. In fact it would correspond to minimum values of the tau neutrino mass included in the allowed region and compatible with structure formation arguments.

The transition from the region with no oscillations to that one with rapid oscillations is very sharp, meaning that the width of the boundary between the two regions is very narrow. In **figure 9** we give an example of this transition for a fixed value of $\delta m^2 = -10\,\text{eV}^2$. Changing the value of $\log(\sin^2 \theta_0)$ for a very small quantity, ~ 0.1, is sufficient to pass from one region to another.

The oscillations take place in a limited interval of temperatures. This interval increases going from points at the border to points in the middle of the rapid oscillations region in the mixing parameter space. This feature again confirms the expectation that the oscillations

are the effect of the breaking of the adiabaticity condition during some period of the lepton number growth and that moving toward the center of the rapid oscillations region, this period becomes longer.

A first observation about the rapid oscillations is that they develop with a temperature period of about $(10^{-3} - 10^{-2})\,\mathrm{MeV}$, depending on the value of $|\delta m^2|$. This period is roughly described by the interval of temperature corresponding to the interaction mean time of neutrinos Γ^{-1} for $x \simeq 2.2$:

$$\Delta_{int}T = \frac{H\,T}{\Gamma} \simeq 2\,\mathrm{MeV}\left(\frac{\mathrm{MeV}}{T}\right)^2 \simeq 5\times 10^{-3}\left(\frac{|\delta m^2|}{\mathrm{eV}^2}\right)^{-\frac{1}{3}}\mathrm{MeV}. \qquad (27)$$

This is in agreement with the expectation for which the coherent nature of the oscillations is damped by the collisions unless the effective potential is rapidly changing.

In the numerical appendix we will show how increasing the resolution in the momentum space for the description of the distributions, has the effect of diminishing the amplitude of the oscillations. For the example in figure 9 with $\sin^2 \theta_0 = 10^{-6.16}$, this effect is such that if the resolution is not high enough, then the amplitude of the oscillations is so large that the total lepton number *changes sign*, while when a good resolution is employed and the numerical solution becomes stable with changing the resolution, the sign changes disappear. If the oscillations are artificially amplified by a numerical error, this can induce the suspect that the sign changes are not a real feature of the solutions. However for a choice of mixing parameters more inside the rapid oscillations region, like already for $\sin^2 \theta_0 = 10^{-6.1}$ in figure 9, it seems that the sign changes do not disappear increasing the accuracy. As we will say in more detail in the appendix, on this point we cannot be conclusive because we cannot reach the required resolution to have perfect numerical stability. It seems that more advanced computational means are necessary to get a definitive conclusion, while in this work we prefer to say that there is an *indication* that the lepton number oscillations change the sign of the solution during the growth regime. We think however that on this point it would be desirable to have some rigorous analytical demonstration, that in our opinion is still missing, even though some attempts have been recently done [14].

Another important problem is whether the final sign of lepton number is sensitive or not to the small statistical fluctuations necessarily present in the early Universe, as we saw in the third section. In our numerical calculations we observe that changes in the initial lepton number are able to change the final sign with a choice of mixing parameters well inside the rapid oscillations region where a large number of oscillations take place. While moving toward the border this effect tends to disappear. This behaviour seems to confirm an effect of 'dephasing' of the solutions as described in [14]. This means that even though solutions with different initial conditions converge at the same values prior the onset of the instability at the critical temperature, (as shown for example in the figure 6), small relic differences will afterwards develop, resulting in growing phase differences during the oscillatory regime and in a possible final sign inversion. However also on this point we cannot be conclusive. It is infact necessary first to get a perfect numerical stability in the description of the neutrino asymmetry oscillations and then to prove that statistical fluctuations as tiny as those present in the early Universe are able to yield a dephasing effect. For this second step it is then necessary that the numerical error is lower than the statistical fluctuations. Thus we cannot

be conclusive because we cannot reach such a computational accuracy. This means also that our analysis cannot neither exclude or demonstrate the possibility of a chaotical generation of lepton domains, but in any case we can say that this possibility is limited to a region of mixing parameters contained in the rapid oscillations region, in a way that the neutrino asymmetry undergoes a number of oscillations high enough that two initially close values of the neutrino asymmetry, result, in the end, in a different final sign. The possibility of drawing the exact contour of such a region, inside the rapid oscillations one, is again something that requires a numerical analysis beyond our present computational means.

We can thus conclude this section saying that the expectation of the appearance of coherent effects on the evolution of lepton number when an adiabatic condition breaks is confirmed by the numerical analysis. This suggests that the oscillations are not just an effect of the numerical error but an intrinsic feature of the equations. The amplitude of these oscillations is much likely large enough to change the sign of the neutrino asymmetry, but on this point we cannot be conclusive, because our maximum accuracy in the description of the momentum dependence is not sufficient to get a good numerical stability and we prefer to speak of indication of sign changes. The demonstration that the changes of sign can induce a chaotical generation of lepton domains is beyond our numerical analysis, but in anycase this can occur only in a region confined within the region of rapid oscillations shown in figure 7. Therefore any application that makes use of a chaotical generation of lepton domains as a general consequence of the QKE, is not justified.

VI. CONCLUSIONS

Large neutrino asymmetry is generated in the early Universe by ordinary - sterile neutrino oscillations for a large range of parameters. We have made a numerical study of the final sign of this asymmetry and our results are summarized in figure 7. In the space of mixing parameters we identified a no oscillation and an oscillation region. In the no oscillation region we could show perfect agreement with the predictions of the static approximation for temperatures $T \stackrel{>}{\sim} T_c$ at which the MSW effect is inhibited by the presence of the collisions. Moreover perfect numerical stability of the solutions was obtained. These two facts do not leave any room for doubt about the generation of a neutrino asymmetry and its final value.

We have also estimated an upper limit [see Eq.(20)] for the size of statistical fluctuations of the lepton number which is very tiny. In view of this, for a choice of mixing parameters in the no oscillation region, the final sign of the neutrino asymmetry is the same in all points of space unless there happens to be larger fluctuations (of non-statistical origin) present. In this way the possibility of a chaotical generation of lepton domains is excluded in the no oscillation region. One consequence of this is that the three neutrino mixing mechanism (proposed in [2]) allowing the $\nu_\mu \leftrightarrow \nu_s$ solution to the atmospheric neutrino anomaly to be consistent with a stringent BBN bound of $N_{BBN}^{eff} < 3.5$ is still viable.

We have also been able to plausibly justify the existence of the rapid oscillations region in terms of a breaking of the static approximation during the lepton number growth.

The study of the rapid oscillations in the oscillation region encounters many numerical difficulties. The oscillations seem to have an amplitude sufficiently large to change the sign of the total lepton number during the growth regime. We however think that further analysis

13

are required to be conclusive on this point. We also think that at the present the numerical analysis cannot neither exclude or demonstrate the possibility of a chaotical generation of lepton domains. This is because the error introduced by the numerical analysis is much larger than the tiny statistical fluctuations present in the early universe. In anycase this possibility is confined to a special choice of the mixing parameters, corresponding to some region contained within the region of rapid oscillations.

Finally we should also mention that while we have focussed on $\nu_\alpha \leftrightarrow \nu_s$ oscillations in isolation, our results will be applicable to realistic models with sterile neutrinos. In the more general case of three ordinary neutrinos and one or more sterile neutrinos, the neutrino asymmetry generation occurs first for the oscillations with the largest $|\delta m^2|$ (with $\delta m^2 < 0$). The sign of this asymmetry (which we assume to be L_{ν_τ} for definiteness) will be the same as $\tilde{L}$ except possibly in the oscillation region where it may depend on δm^2, $\sin^2 2\theta_0$. The other oscillations with smaller $|\delta m^2|$ may also generate significant neutrino asymmetry, although this generation occurs latter on (see e.g. Ref. [3,7] for some examples). The sign of these asymmetries will ultimately depend only on the sign of L_{ν_τ} since this dominates $\tilde{L}$ for these oscillations.

NUMERICAL APPENDIX

In this Appendix we want to describe in more detail our numerical procedure for solving the QKE's. As we said already in the text we employed two different codes, one using the thermal equilibrium assumption (*code A*), the other using the expression (6) for the repopulation account (*code B*). The code B has been already described in [4] and we refer the reader to this reference for details. Here we describe common features of the two and specifications of the code A.

We first discuss the time step and then the momentum integration is described.

The time step of integration is adjusted in a way that it is halved until the required accuracy (the relative error on all the set of variables of the system) ϵ is reached. By this we mean that for each variable we introduce a time step Δt. At every time step during the evolution, say at $t = t_x$ we compute $Z(t_x + \Delta t)$ and compare this with the results of integration with a half step size, symbolically, $Z(t_x + \Delta t/2 + \Delta t/2)$. Explicitly, the step size is halved until every integration variable (which we have denoted collectively as Z) satisfies,

$$|Z(t_x + \Delta t) - Z(t_x + \Delta t/2 + \Delta t/2)| < \epsilon |Z(t_x + \Delta t) + Z(t_x + \Delta t/2 + \Delta t/2)|/2. \qquad (28)$$

The above procedure is quite standard, and is called Merson' s procedure' or *step doubling* [24,25] and together with a fourth order Runge-Kutta solver is considered the most straightforward and safe technique [8].

―――――

[8] An evolution of this procedure is given by the "Fehlberg" or *embedded Runge-Kutta method*. This method should be twice as fast as Merson's one and although it should be safe enough, we have adoped the more conservative Merson's procedure for code A. Another possibility is offered by the Bulirsch-Stoer method that is by far the most efficient but it has many cautions for its usage.

We now discuss the discretization of momentum and the integration around the resonances procedure. The range of values of momenta (p/T) is $[x_1, x_N]$ which is discretized on a logarithmically spaced mesh:

$$x_j = x_1 \times 10^{(j-1)\Delta}, \; j = 1, 2, ..., N \tag{29}$$

where N is the number of bins and $\Delta \equiv \log(x_N/x_1)/(N-1)$. The initial temperature is chosen in a way that the initial resonant momentum is x_{in}.

The resonance momentum for neutrinos, $x_{res} \equiv p_{res}/T$ can be obtained by solving $\lambda(x) = 0$ [with $\lambda(x)$ defined in Eq.(11)] and is given by

$$x_{res} = \frac{X_2}{2X_1} + \sqrt{\left(\frac{X_2}{2X_1}\right)^2 + \frac{c}{X_1}}, \tag{30}$$

where $c \equiv \cos 2\theta_0$ and $X_1 \equiv b/x^2, X_2 \equiv a/x$ [recall a, b are defined in Eq.(12)]. Note that $X_{1,2}$ are independent of x. The resonance momentum for antineutrinos can be obtained by replacing $X_2 \to -X_2$ in the above equation. The width of the resonance is given by the following expression [9]:

$$\delta x = 2 \left[\frac{\sqrt{\sin^2 2\theta_0 + d_0^2 b^2}}{c + b} \right]_{x_{res}} x_{res} \equiv \delta_{res} x_{res}, \tag{31}$$

where we introduced the *logarithmic width of the resonance* $\delta_{res} = \delta \ln x$ and $d_0 \equiv 2p_{res}D/b\delta m^2$. Numerically, $d_0 \simeq 2 (0.8) \times 10^{-2}$, for $\alpha = \mu, \tau$ (e). Note that δ_{res} is roughly independent of T for $T \gtrsim T_c$ (and is of order d_0) while for $T \ll T_c$, δ_{res} decreases to $\sim \sin 2\theta_0$. It is also roughly independent of the momentum x and this is the reason for which it is more convenient to use a logarithmically spaced mesh rather than a linearly spaced one.

At each step of integration we calculate both x_{res} and δ_{res} and we discretize them: $x_{res} \to j_{res}$ with

$$j_{res} = Int \left[\frac{1}{\Delta} log \frac{x_{res}}{x_1} \right] + 1 \tag{32}$$

and we define $\Delta j \equiv 1 + \text{Int}(\delta_{res}/\Delta)$. Considering that $\delta_{res} = \delta(\ln x) \simeq 2.3 \times \delta \log x$, this means that Δj corresponds roughly to twice the width of the resonance in a logarithmic scale and in units of Δ. At each time step we integrate only on those bins among $[1, N]$ in the interval $[j_{min}, j_{max}]$ where:

Same considerations hold for predictor-corrector methods that are considered somehow worse than all of the previous ones. As we had to study unexplored features of still 'young' equations, we preferred to adopt the *step doubling* method (see [25] for further details).

[9]This is derived in Ref. [4]. The form given in Eq.(31) is simpler, but mathematically equivalent to Δ/p_{res} where Δ is given in Eq.(28) of Ref. [4].

$$j_{\min} = j_{\text{res}} - \rho\,\Delta j, \quad j_{\max} = j_{\text{res}} + \rho\,\Delta j \qquad (33)$$

In this way we are integrating symmetrically around the resonance (we are taking equal numbers of bins with lower and higher momenta), but logarithmically, while in the code B this is done linearly [4]. Clearly $j_{\min}$ and $j_{\max}$ are constrained within $[1, N]$. This procedure is done at each step so that the interval of integration follows dynamically the resonance. Initially the neutrino and anti-neutrino resonances approximately coincide due to the approximate fixed point $L^{(\alpha)} \approx 0$. However during the exponential growth the resonance splits in two, one at low momenta for the antineutrinos and one at high momenta for the neutrinos if $L^{(\alpha)} > 0$ or vice versa if $L^{(\alpha)} < 0$. The split occurs gradually: first the initial interval enlarges and at certain point it splits, so that eventually the two intervals do not overlap.

Let us introduce the number of bins which we integrate over, which for neutrinos we denote by M_ν and is given by $M_\nu \equiv \min(N, J_{\max}) - \max(1, J_{\min})$ (and similarly for antineutrinos we introduce the quantity $M_{\bar\nu}$). So at each step of integration we solve a system of $3(M_\nu + M_{\bar\nu}) + 1$ equations in the code A and $4(M_\nu + M_{\bar\nu}) + 1$ in the code B.

In this way one has 6 numerical parameters: $\epsilon, x_1, x_N, x_{in}, \rho, N$. One has to check carefully that the numerical solution is 'stable' changing these parameters in the direction of greater accuracy.

For the parameter ϵ we checked that $\epsilon = 10^{-4}$ is a safe value. A safe choice for (x_{in}, x_1, x_N) is $(0.1, 10^{-3}, 20)$ [$x_{in} = 0.1$ corresponds approximately to the choice $T_{in} \simeq 3 \times T_c$ where T_c is given by Eq.(18)].

The minimum value for N to get an accurate description, depends on the values of the mixing parameters, whether they are outside or inside the rapid oscillations region. The number of bins N, necessary to have a stable solution, is that one for which the number of bins within a width of resonance, Δj, is large enough. A value $\Delta j \sim 10$, that corresponds to $N \sim 2^{11}$, is sufficient in the no oscillatory region to have stable solutions as shown in **figure 10a**.

A first observation concerning the value of ρ to be chosen is that $\rho \sim 100$ corresponds roughly to integrate on all the range of momenta $10^{-3} - 20$ [10]. For values of mixing parameters in the no oscillation region, $\rho = 4$ is a good choice in order to study the problem of sign. In **figures 10a, 10b** we present the result of a check that shows the numerical stability of our results for the indicated values of the mixing parameters. In figure 10a the mixing parameters correspond to a point close to the border with the rapid oscillations region.

More precisely the minimum value of ρ to get the stability, in the no oscillations region, depends on the initial value of the total lepton number. If one choose $L_{in}^{(\alpha)} = 0$, a relative low value of $\rho = 4$ is sufficient to get a full stability at all temperatures in an impressive way.

_____

[10]If we start from $x_{in} = 0.1$ and if we consider the case $\alpha = \mu, \tau$ so that $\delta_{res} \simeq d_0 \simeq 0.02$ (for $T \overset{>}{\sim} T_c$), then the choice $\rho = 100$ is equivalent to integrating on the interval $10^{-3} < x < 10$. At the critical temperature $x_{res} \approx 2$, the integration interval moves at values $0.02 < x < 20$. This means that the integration around the resonance is not necessarily more approximated than the case when a *static* interval of integration is chosen, it is simply a way to select a reduced interval of momenta but dynamically, taking into account the resonant behaviour of the process.

On the other hand if one starts from non vanishing values of the initial lepton number, the approximation of integrating around the resonance gives an error at high temperatures, in the regime during which the lepton number is destroyed. This is also clearly shown in figure 10a and 10b for the indicated mixing parameters. This fact has already been described and justified in the main text.

In the oscillatory region, in order to get stability, the necessary number of bins inside a resonance width seems to hugely increase upto about $\Delta j \simeq 500$, obtained for $N \simeq 2^{17}$, as shown in **figures 11a, 11b**. It is remarkable to notice how an inaccurate description of the momentum dependence amplifies the amplitude of the oscillations and for $\sin^2 2\theta_0 = 10^{-6.16}$ it makes the solution changing sign. However for an higher value of the mixing angle the sign changes are present also when the maximum accuracy is employed. The stability of the solutions in the oscillatory regime is clearly not as good as outside this regime, even though there is still some indication on the behaviour of the solutions. Not only it would be desirable to make checks increasing the number of bins N, but also increasing the width of the region of integration around the resonance, that means the parameter ρ. Unfortunately this is not possible not only because the required computational time becomes too long, but also because the dimensions of the arrays employed to describe the distributions requires an amount of RAM memory than our machines do not have. It would be also desirable to make checks increasing the numerical precision, in our case passing from a double precision (the round off error is about 10^{-16}) to a quadruple precision. This because at the onset of the instability the rate of growth of neutrino asymmetry is the difference of two opposite quantities that are much higher. Unfortunately we do not have at the moment the possibility to perform quadruple precision runs, also because again the time for the runs becomes too long. For all these reasons we prefer to speak of a strong 'indication' that the oscillations are able to change the sign of the neutrino asymmetry.

In the end of this appendix we want to mention that also for an accurate evolution at low temperatures $T \ll T_c$, large values of N are required (depending on $\sin 2\theta_0$). This is because, the resonance width becomes quite narrow at low temperatures [see the discussion above, following Eq.(31)].

This appendix has been stimulated by the scepticism expressed in [10] about the numerical procedure employed in the previous existing works dealing with the numerical solutions of the exact QKE. It should be clear now that the results and the procedure were already rigorous at that time, just there was not a compelling necessity to provide all the tedious details as we do now.

REFERENCES

[1] R. Foot, M. J. Thomson and R. R. Volkas, Phys. Rev. D53, 5349 (1996).

[2] R. Foot and R. R. Volkas, Phys. Rev. D55, 5147 (1997).

[3] R. Foot and R. R. Volkas, Phys. Rev. D56, 6653 (1997); Erratum-ibid, D59, 029901 (1999).

[4] R. Foot, Astropart. Phys. 10, 253 (1999).

[5] N. F. Bell, R. R. Volkas and Y.Y.Y.Wong, Phys. Rev. D59, 113001 (1999).

[6] P. DiBari, P. Lipari and M. Lusignoli, hep-ph/9907548.

[7] For BBN implications of the neutrino asymmetry in various 4 and 6 neutrino models, see Ref. [2–4,6] and also N. F. Bell, R. Foot and R. R. Volkas, Phys. Rev. D58, 105010 (1998); R. Foot, hep-ph/9906311 (to appear in Phys. Rev. D). For applications to models with mirror neutrinos, see R. Foot and R. R. Volkas, Astropart. Phys. 7, 283 (1997); hep-ph/9904336 (to appear in Phys. Rev. D).

[8] K.Enqvist, K.Kainulainen and J.Maalampi, *Nucl.Phys.* B349 754 (1991); R.Barbieri and A.D. Dolgov, *Nucl.Phys.* B349 743 (1991).

[9] D.P. Kirilova and M.V. Chizhov, Nucl.Phys. B 534, 447 (1998).

[10] A.D.Dolgov, S.H.Hansen, S.Pastor and D.V.Semikoz, hep-ph/9910444.

[11] X. Shi and G. Fuller, *Phys.Rev.Lett.* 83, 3120 (1999).

[12] X. Shi, Phys. Rev. D54, 2753 (1996).

[13] K. Enqvist, K. Kainulainen and A. Sorri, Phys. Lett. B464, 199 (1999).

[14] A. Sorri, hep-ph/9911366.

[15] R. A. Harris and L. Stodolsky, Phys. Lett. 116B, 464 (1982); Phys. Lett. B78, 313 (1978); A. Dolgov, Sov. J. Nucl. Phys. 33, 700 (1981).

[16] B. H. J. McKellar and M. J. Thomson, Phys. Rev. D49, 2710 (1994).

[17] L. Stodolsky, Phys. Rev. D36, 2273 (1987); M. Thomson, Phys. Rev. A45, 2243 (1991).

[18] K. Enqvist, K. Kainulainen and M. Thomson, Nucl. Phys. B 373, 498 (1992).

[19] L. Wolfenstein, Phys. Rev. D17, 2369 (1978).

[20] D. Notzold and G. Raffelt, Nucl. Phys. B307, 924 (1988).

[21] K. Enqvist, K. Kainulainen and J. Maalampi, Phys. Lett. B244, 186 (1990).

[22] P. Di Bari, hep-ph/9911214.

[23] R. Foot and R. R. Volkas, Phys. Rev. Lett. 75, 4350 (1995).

[24] G. N. Lance, 'Numerical methods for high speed computers' (London 1960).

[25] W.H. Press, S.A.Teukolsky, W.T.Vetterling and B.P. Flannery, 'Numerical Recipes, the Art of Scientific Computing', Cambridge University Press (1994).

FIGURE CAPTIONS

Fig. 1 Evolution of the effective total lepton number, $L^{(\tau)}$, for $\nu_\tau - \nu_s$ oscillations for the parameter choice, $\delta m^2 = -10 \ eV^2$, $\sin^2 2\theta_0 = 10^{-7}$. In Fig.1a, the solid line is the numerical solution of the QKEs, Eq.(6) integrating around the resonances using $f = 12$ resonance widths and in a linearly symmetric way (the 'code B' has been used: see the Appendix and [4] for its definition), while the dashed line is the static approximation (described in the text) also integrating around the resonance. Fig.1b is a comparison of the static approximation

integrating around the resonance (solid line) with integrating over the entire momentum range $0.01 < p/T < 20$ (dashed line). Note that $\tilde{L} = 5 \times 10^{-10}$ is used and the initial value of L_{ν_τ} is zero in this example.

Fig.2a,b Same as figures 1a,b except that the oscillation parameters are changed to $\delta m^2 = -100 \ eV^2$, $\sin^2 2\theta_0 = 10^{-8}$.

Fig. 3 Numerical solution of the QKE's (solid line) integrated over the entire momentum range $0.1 < x < 12$ for the parameter choice $\delta m^2 = -0.01 \ eV^2$, $\sin^2 2\theta_0 = 10^{-7}$. The initial value of L_{ν_τ} is zero in this example. Also shown is the static approximation integrated over the same momentum range and same initial conditions (dashed line).

Fig. 4a,b High temperature evolution of the effective total lepton number, $L^{(\tau)}$, for $\nu_\tau - \nu_s$ oscillations. Figure 4a is for the parameter choice, $\delta m^2 = -1 \ eV^2$, $\sin^2 2\theta_0 = 10^{-7}$ (with $L^{(\tau)}_{initial} = \tilde{L} = 5 \times 10^{-10}$, i.e. initial $L_{\nu_\tau} = 0$) while figure 4b is for $\delta m^2 = -10 \ eV^2$, $\sin^2 2\theta_0 = 10^{-7}$ (with $L^{(\tau)}_{initial} = 10^{-12}$). The solid line is the numerical solution of the QKEs, Eq.(6), while the dashed line is the solution of the QKEs assuming a thermal distribution for the active neutrino (as discussed in the text).

Fig. 5 An example of the high temperature evolution of the effective total lepton number, $L^{(\tau)}$ for $\delta m^2 = -10 \ eV^2$ for $\sin^2 2\theta_0 = 10^{-9}$ (dotted line), 10^{-8} (dashed line) 10^{-7} (solid line).

Fig. 6 An example of the high temperature evolution of the effective total lepton number, $L^{(\tau)}$ for $\delta m^2 = -10 \ eV^2$ for $\sin^2 2\theta_0 = 10^{-7}$ with the initial values of L_{ν_τ} given by $L_{\nu_\tau} = 10^{-10}$ (solid line), 10^{-9} (long dashed line), 10^{-8} (short dashed line), 10^{-7} (dotted line).
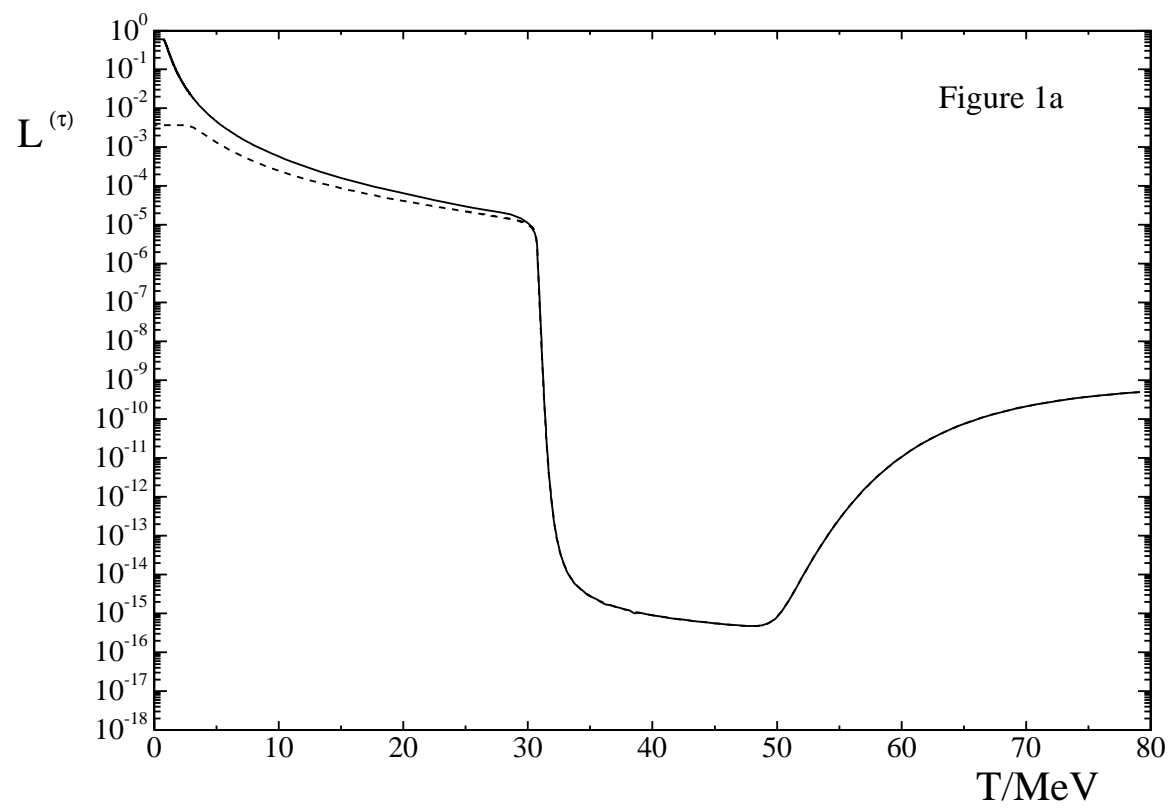
Fig. 7 Region of parameter space where the final sign does and does not oscillate for $\nu_\tau \leftrightarrow \nu_s$ oscillations. Also shown is the 'allowed region' (which we define below) for the $\nu_\mu \leftrightarrow \nu_s$ maximal oscillaton solution to the atmospheric neutrino anomaly. This is the region where the L_{ν_τ} is generated rapidly enough so that the sterile neutrino is not equilibrated by either $\nu_\mu \leftrightarrow \nu_s$ maximal oscillations (region above the dashed-dotted line) or by $\nu_\tau \leftrightarrow \nu_s$ oscillations (region to the left of the dotted line).
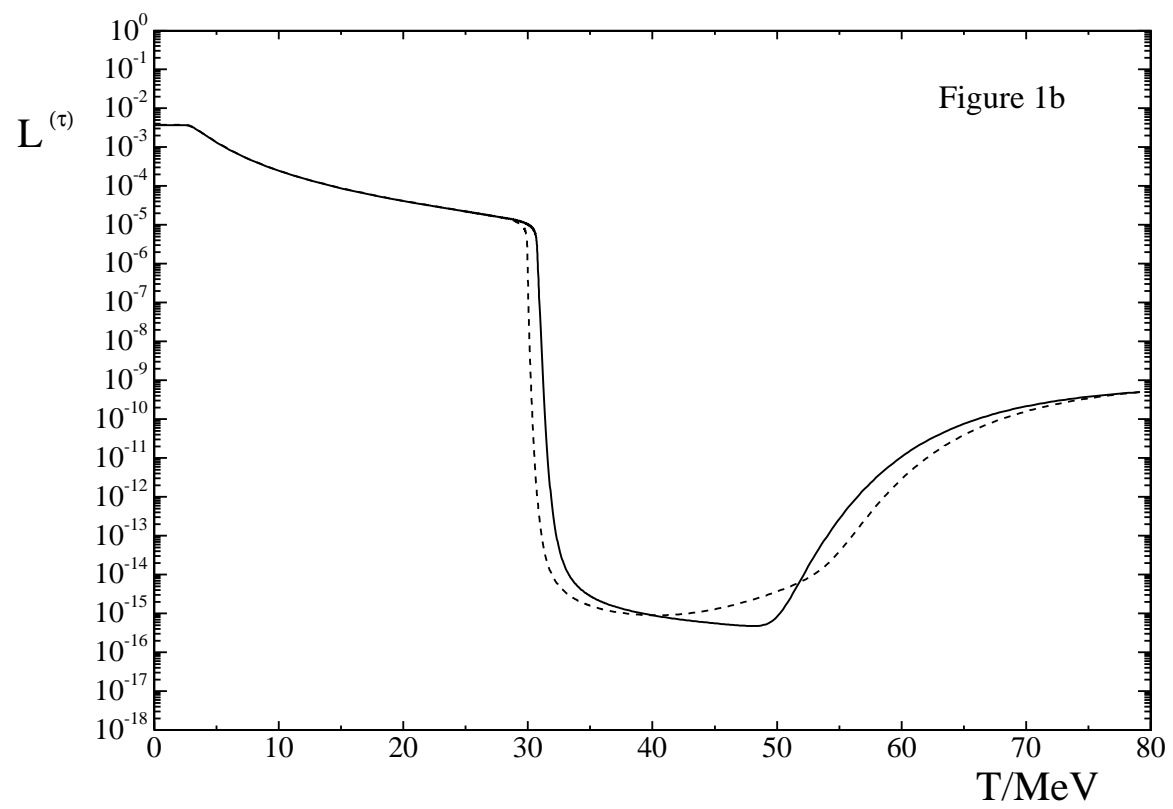
Fig. 8 The evolution of the total lepton number for a choice of mixing parameters just outside the top of the rapid oscillations region. The sterile neutrino production increases with the mixing angle. It appears clear the double effect of the sterile neutrino production in delaying the onset of the growth, lowering the critical temperature and in depressing the rate of growth of lepton number. The latter prevents the arise of rapid oscillations when the mixing angle increases.
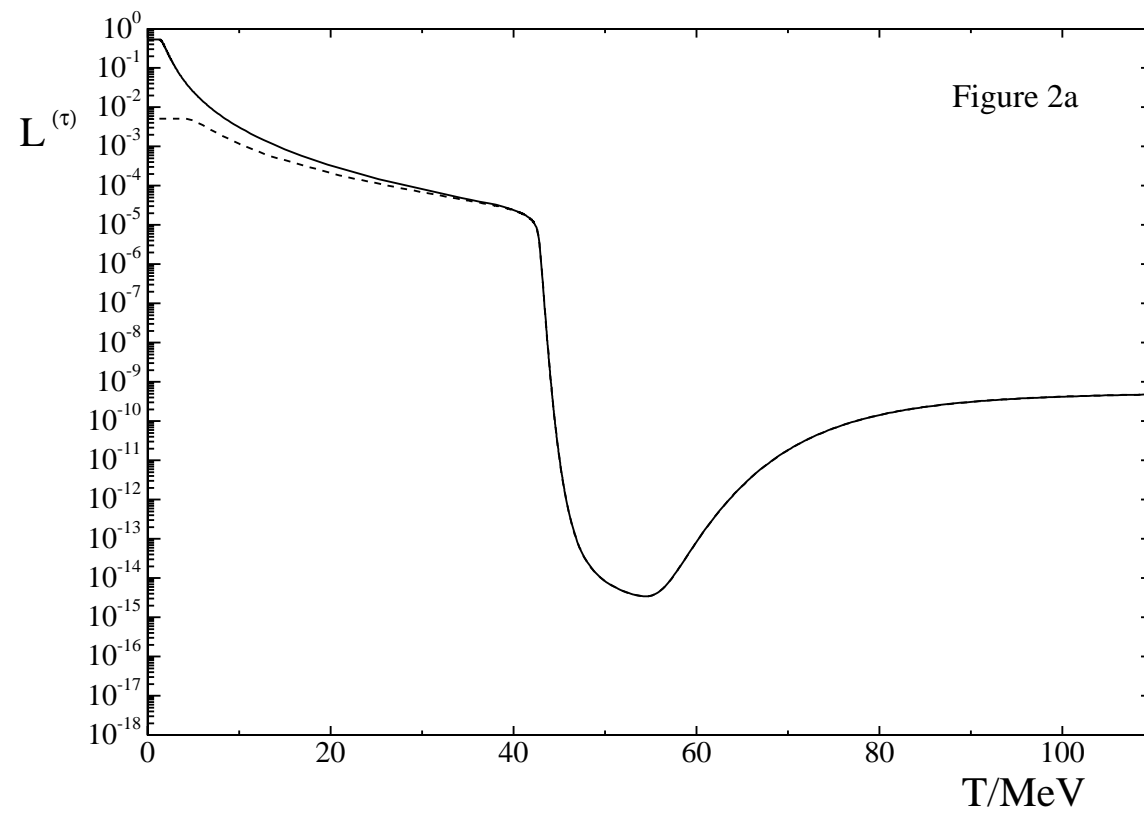
Fig. 9. Transition from the no oscillations region to the rapid oscillation region increasing the value of the mixing angle for a fixed value of $\delta m^2 = -10 \ eV^2$.
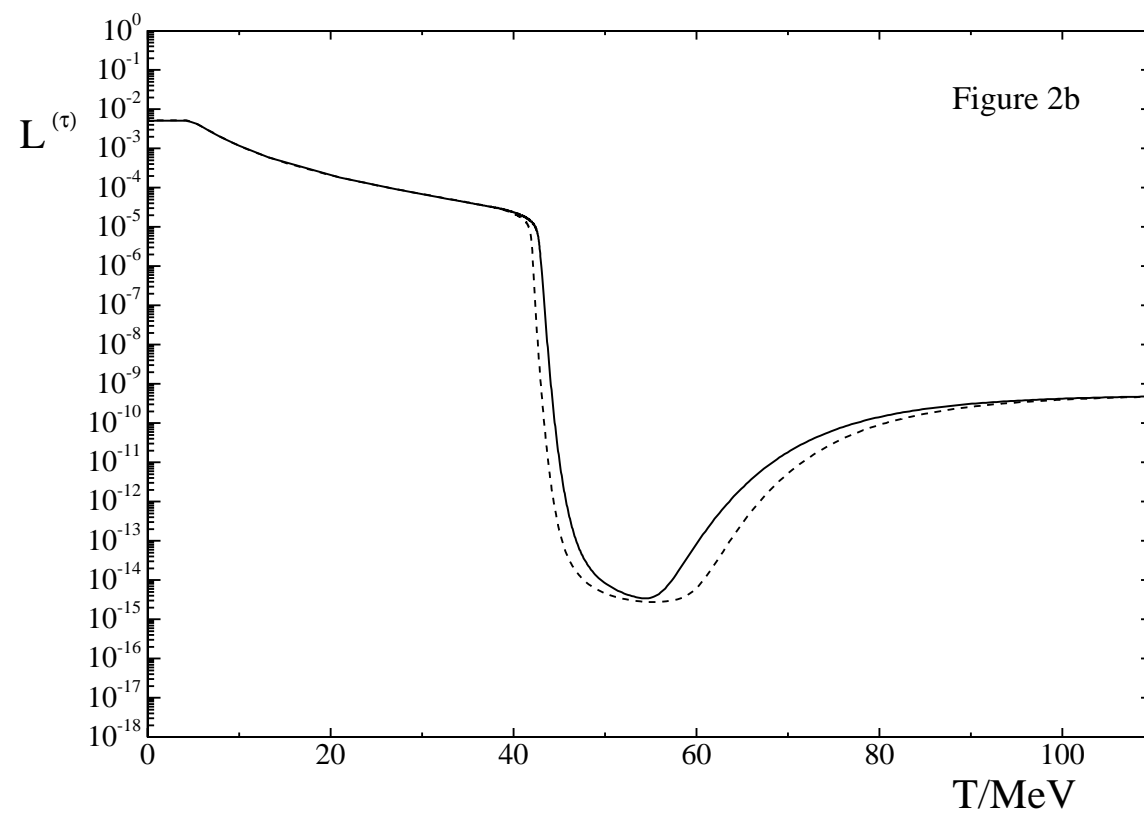
Fig. 10 Check of numerical stability for two different choices of mixing parameters inside the no oscillation region for $\delta m^2 = -10 \ eV^2$ and $\sin^2 2\theta_0 = 10^{-6.2}$ (a), $\sin^2 2\theta_0 = 10^{-7}$ (b). It appears clear the validity of the resonant approximation in this region when $L^{(\alpha)}_{in} = 0$. On the other hand for $L^{(\alpha)}_{in} = \tilde{L} = 5 \times 10^{-11}$, the resonant approximation produces an error in the regime of high temperatures ($T \gg T_c$) when the initial lepton number is destroyed.
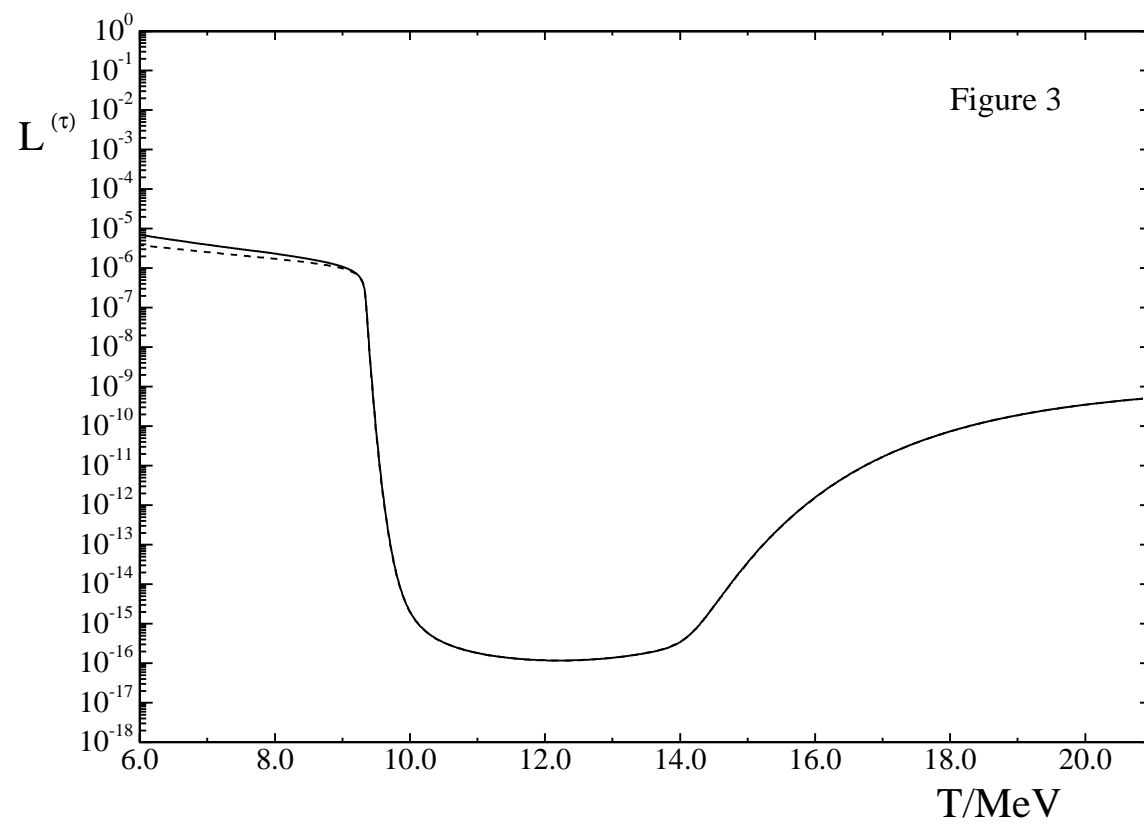
Fig. 11 Check of numerical stability in the oscillatory regime for $\delta m^2 = -10 \ eV^2$ and $\sin^2 2\theta_0 = 10^{-6.16}$ (a), $\sin^2 2\theta_0 = 10^{-6.2}$ (b).
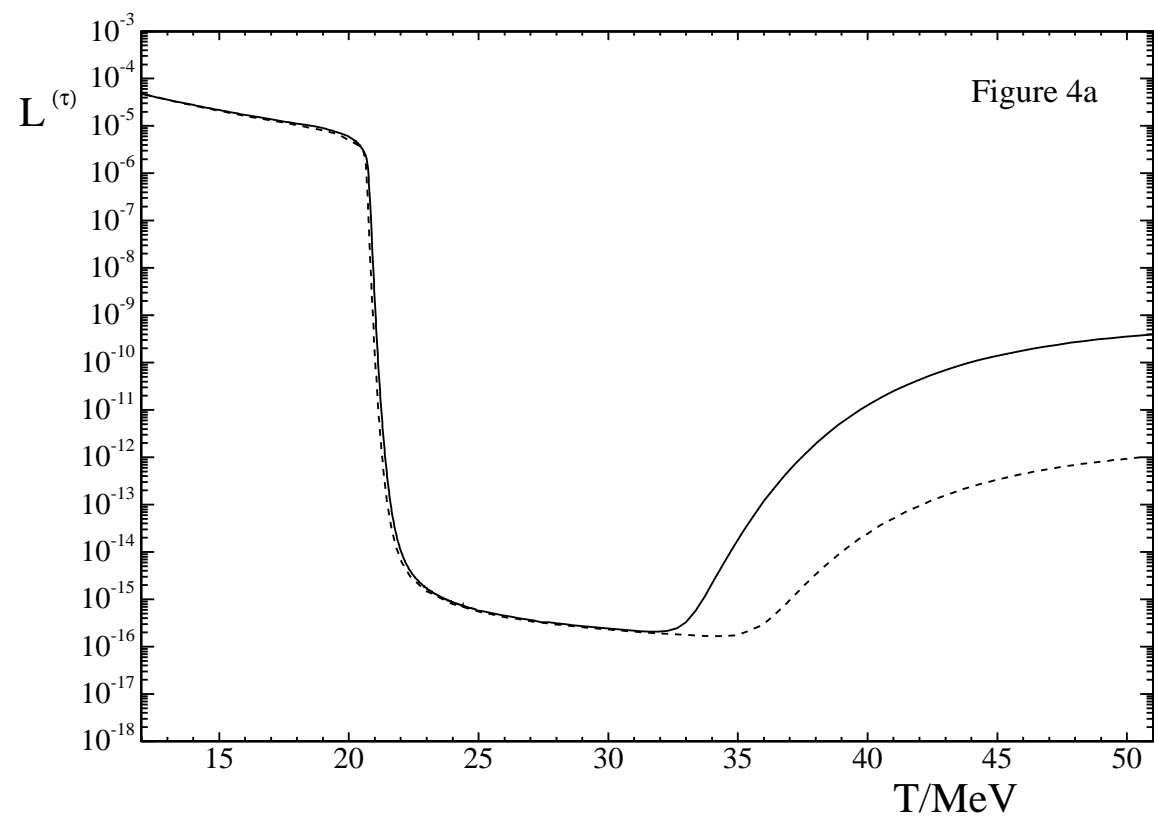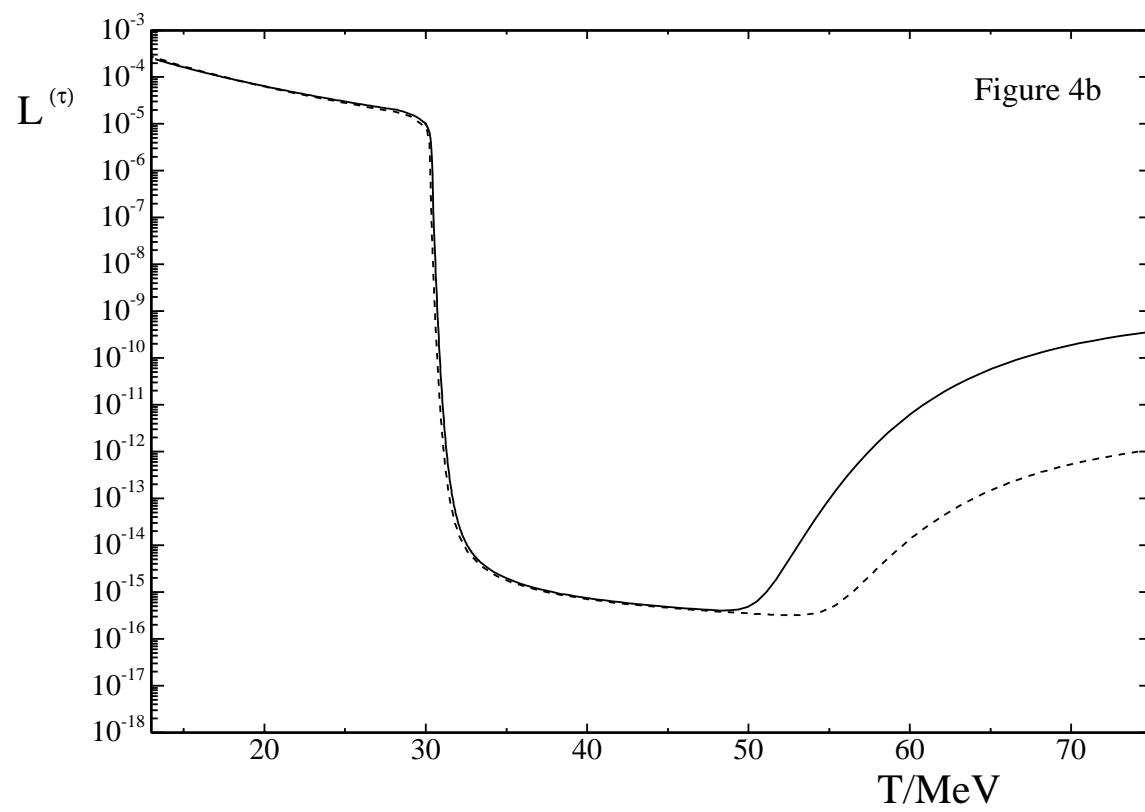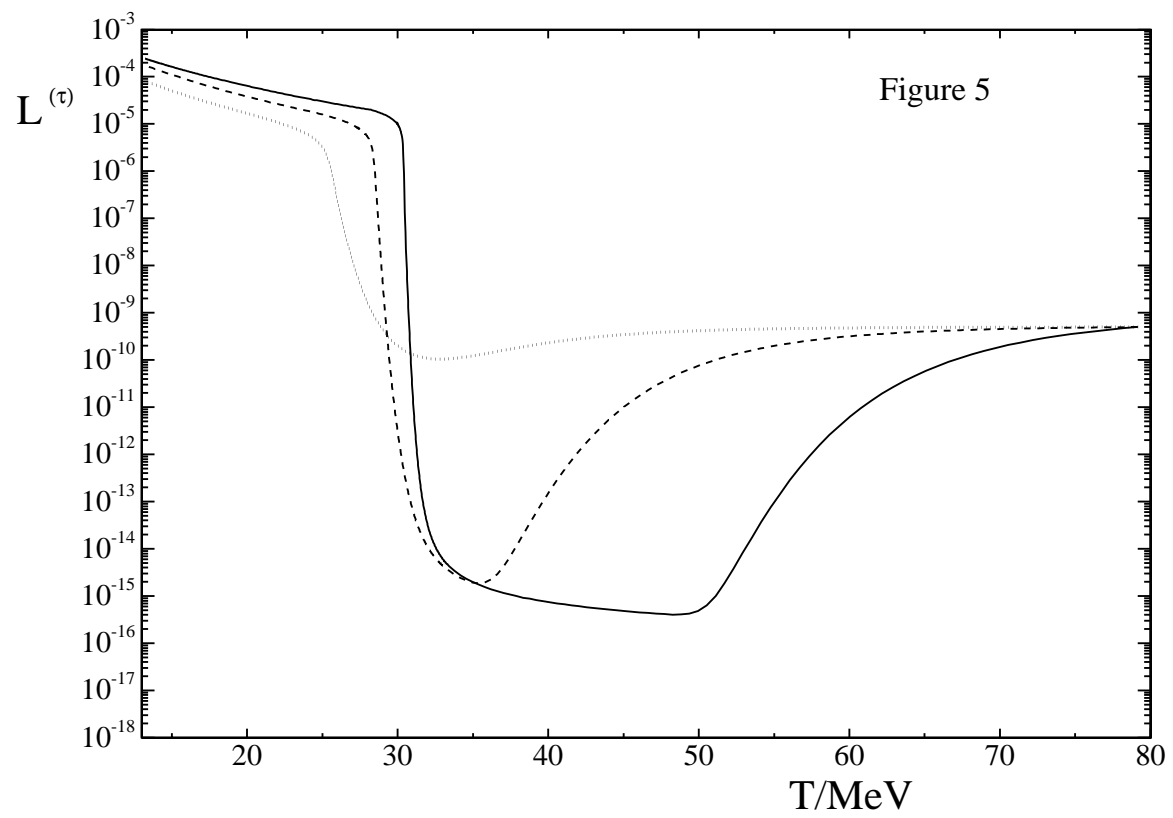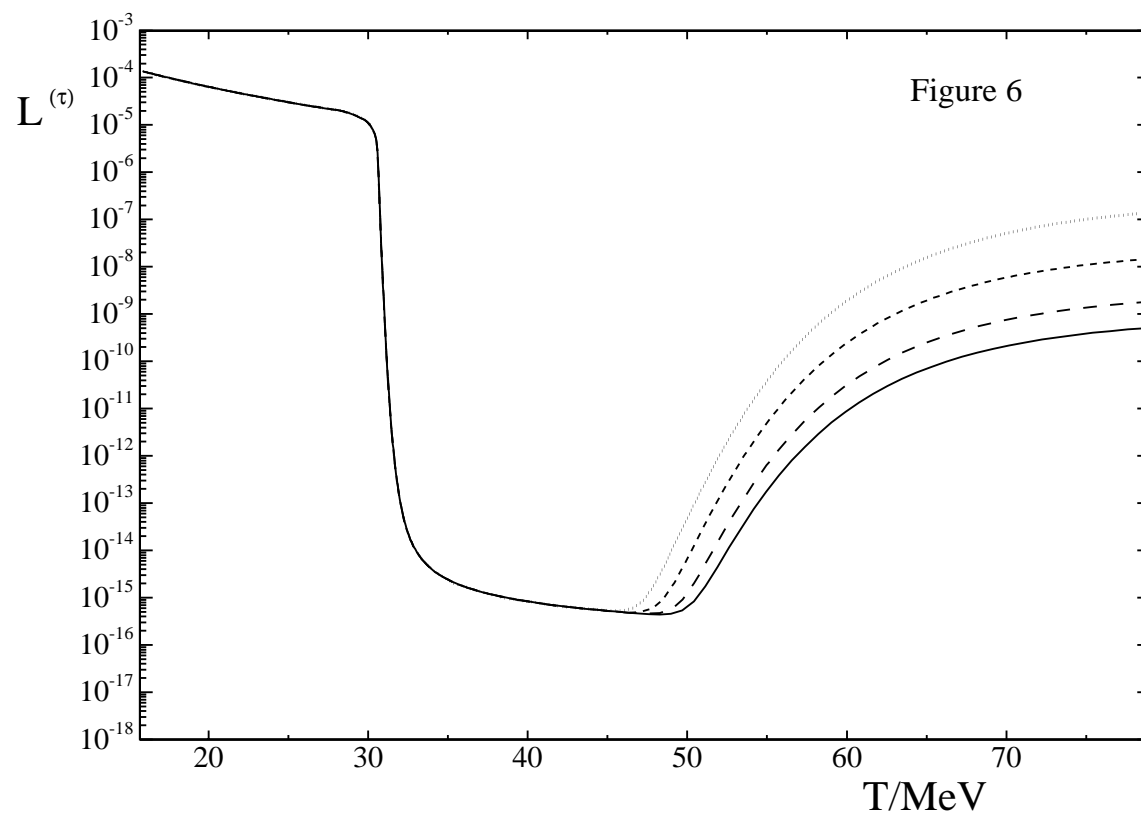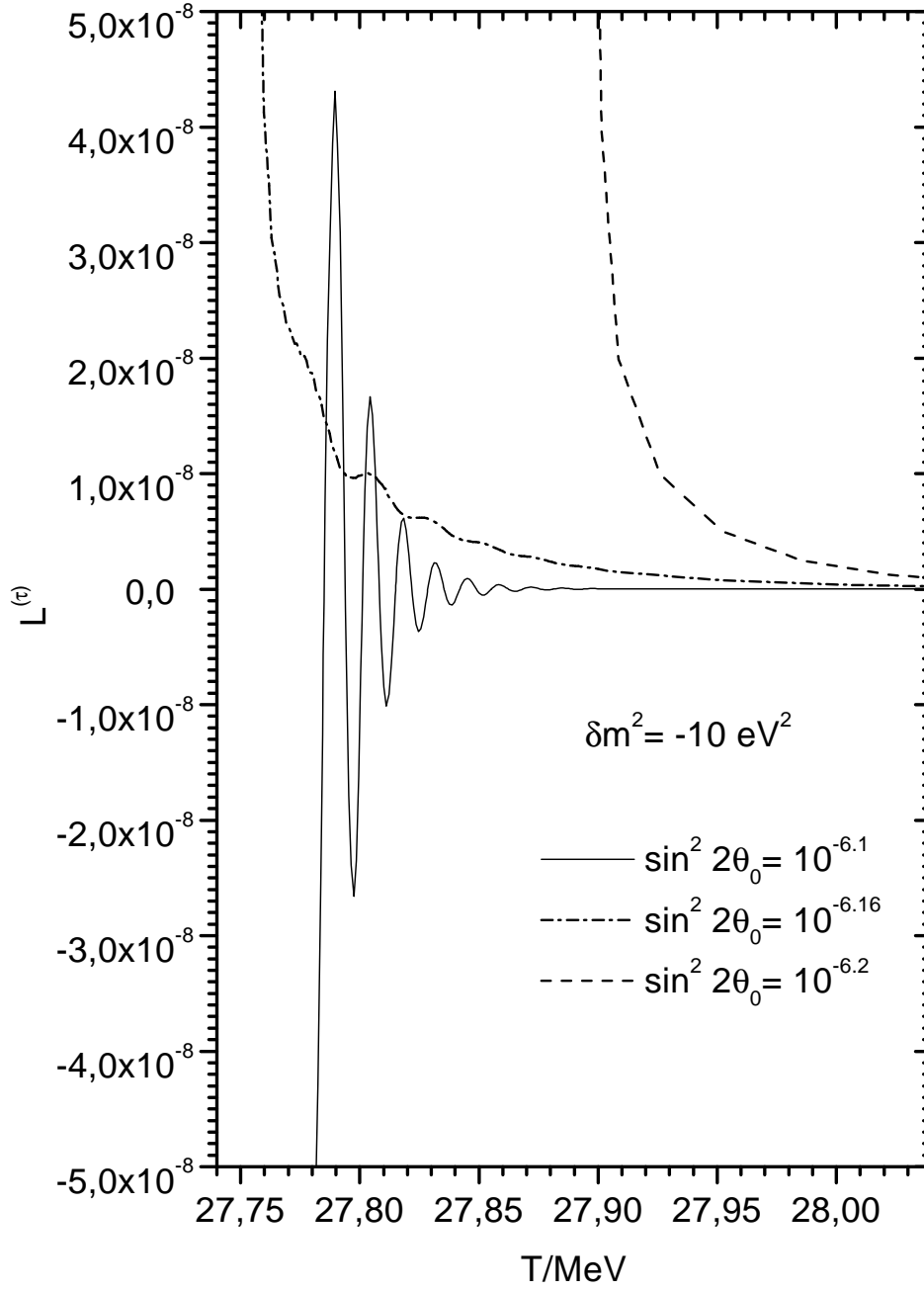
Figure 1a

Figure 1b

Figure 2a

Figure 2b

Figure 3

Figure 4a

Figure 4b

$L^{(\tau)}$

T/MeV

Figure 5

figure 7

$-\delta m^2 / eV^2$

$\sin^2 2\theta_0$

N O

OSCILLATIONS

RAPID

OSCILLATIONS

(?)

figure 8

$\delta m^2 = -10^{2.7}\ eV^2$

$s^2 = 10^{-6.1}$
$s^2 = 10^{-6.0}$
$s^2 = 10^{-5.9}$
$s^2 = 10^{-5.8}$

$L^{(\tau)}$

$T\ /\ MeV$

figure 9

figure 10a

$\delta m^2 = -10\ eV^2$

$\sin^2 2\theta_0 = 10^{-6.2}$

	$\varepsilon=10^{-4}$	$\rho=4$	$N=2^{11}, 2^{13}$
	$\varepsilon=10^{-8}$	$\rho=4$	$N=2^{11}, 2^{13}$
	$\varepsilon=10^{-4}$	$\rho=8$	$N=2^{11}, 2^{13}$
	$\varepsilon=10^{-4}$	$\rho=16$	$N=2^{11}, 2^{13}$
	$\varepsilon=10^{-4}$	$\rho=32$	$N=2^{11}, 2^{13}$
	$\varepsilon=10^{-4}$	$\rho=40$	$N=2^{11}, 2^{13}$

$L^{(\tau)}$

T / MeV

figure 10b

$\delta m^2 = -10 \text{ eV}^2$

$\sin^2 2\theta_0 = 10^{-7}$

$\varepsilon = 10^{-4} \quad N = 2^{11}$

$\rho = 4$
$\rho = 8$
$\rho = 16$
$\rho = 32$
$\rho = 40$

$L^{(\tau)}$

T/MeV

figure 11a

$\sin^2 2\theta_0 = 10^{-6.16}$

$\delta m^2 = -10 \text{ eV}^2$

$\varepsilon = 10^{-4} \quad \rho = 4$

$L^{(\tau)}$

T/MeV

$N = 2^{12}$
$N = 2^{14}$
$N = 2^{16}$
$N = 2^{17}$

figure 11b

$\sin^2 2\theta_0 = 10^{-6.1}$

$\delta m^2 = -10 \text{ eV}^2$

$\rho = 4$ $\varepsilon = 10^{-4}$

$N = 2^{12}$
$N = 2^{14}$
$N = 2^{16}$
$N = 2^{17}$

$L^{(\tau)}$

T/MeV